Q. J. R. Meteorol. Soc. (2005), **128**, pp. 1–999 doi: 10.1256/qj.yy.n

Use of Potential Vorticity for Incremental Data Assimilation

By M. WLASAK[1]*, N. K.NICHOLS[1] AND I. ROULSTONE[2]
[1]*Department of Mathematics, University of Reading, U. K.*
[2]*Department of Mathematics, University of Surrey, U. K.*

(Received 1 January 2005; revised ???)

Summary

Decomposing the mass and wind fields in a data assimilation scheme into balanced and unbalanced flow is part of the process of defining a covariance model. It is not uncommon to assume that the dynamic balanced part of the flow is approximated solely by the rotational part of the wind, which is obtained from a Helmholtz decomposition of the horizontal momentum (with an associated balanced pressure being diagnostically inferred from a balance equation, for example). The unbalanced flow is then represented by the divergence and the residual unbalanced pressure. The assumption that the rotational part of the momentum is a good approximation to the total balanced flow is only valid in certain regimes. We propose a new approach that incorporates flow regime dependence, where we assume that the balanced part of the flow is approximated instead by a linearised potential vorticity increment. We show the benefit of such a formulation in the context of shallow water equations defined on a hemisphere.

Keywords: Potential Vorticity Data Assimilation Linearisation Rossby-Haurwitz Waves Burger number Incremental

1. Introduction

Lorenc (2003, §3(b)) points out that physical arguments are frequently used to select a set of variables (so-called 'control variables' in Numerical Weather Prediction (NWP)) for use in data assimilation schemes, which decompose atmospheric states into balanced and unbalanced components. Such variables enable the background error covariances to be more readily applied than would be the case if, for example, the usual model variables of momentum and pressure were used. Most numerical weather centres that perform data assimilation represent the balanced and unbalanced parts of the flow in a simplified, flow independent fashion that assumes that the balanced flow is just the rotational part, with the associated balanced pressure field derived using a linear balance equation. The 'fast modes' (i.e. the gravity wave activity) are represented by the divergence and a residual unbalanced pressure. While it is true that the balanced flow is predominantly rotational, choosing the rotational wind as the 'slow variable' is only applicable in flow regimes where the Rossby radius of deformation is significantly larger than the characteristic horizontal length scale. In reality, this assumption breaks down at planetary length scales where the horizontal length scale is very large or where the Rossby radius of deformation is small due to buoyancy effects (etc). To incorporate these effects we need a simple scheme that has some flow regime dependency. An efficient scheme is needed so that this part of the data assimilation process does not cost significantly more computationally than at present, and this is an important constraint in schemes that may involve solving complicated elliptic boundary value problems.

We propose to use a low order potential vorticity (PV) inversion scheme to select a set of control variables that separate the balanced and unbalanced components of the flow in a more flow dependent manner. We make the assumption that the potential vorticity contains the balanced part of the flow, and that the unbalanced flow lies in the kernel of the PV operator (i.e. that flow with

* Corresponding author: Met Office, FitzRoy Road, Exeter EX1 3PB, U.K.

PV=0). McIntyre and Norton (2000) discuss various hierarchical approximations to potential vorticity inversion on a hemisphere within a shallow water context. We propose a PV inversion scheme that is similar to their first order direct inversion scheme, except that we use the linear balance equation instead of Charney balance as our associated balance condition. We also work with a linearisation of the potential vorticity because our scheme is designed to work with incremental data assimilation schemes. Our PV inversion scheme is consistent with the shallow water equations linearised about a resting state.

We discriminate between different flow regimes by using the Burger number. This is a measure of the stable stratification of a fluid: when the Burger number is low, the height, or depth, is an appropriate measure of the balanced component of the flow; but when the Burger number is high, the vorticity is the appropriate measure. Another way of saying this is to note that the PV behaves like the reciprocal of the height at low Burger numbers and like the vorticity at high Burger numbers. Therefore, in our application in data assimilation, the PV should be a better representation of the balanced flow where and when the Burger number is small, while giving approximately similar results to the vorticity when the Burger number is large.

We present theoretical and numerical aspects of this PV inversion and show the benefits of such a scheme when compared to a scheme in which the balanced component is represented by the rotational flow. In section 2 we present the theoretical aspects, giving a rationale for using potential vorticity within a shallow water context. We show how the relative contributions to scaled potential vorticity perturbations vary with Burger number. In section 3 we state the numerical method that is used and section 4 we present the numerical results.

2. Theory

(*a*) *Introduction*

In this section we explain why we want to use a potential vorticity (PV) inversion scheme in data assimilation to separate the key dynamical aspects of the flow. Most operational centres use just the rotational and divergent parts of the flow for this purpose. It is our aim to show that using a PV inversion scheme is a more consistent approach as it takes account of the regime dependence of the flow.

The first step is to establish the standard rationale for using the streamfunction ψ, a scalar quantity representing the rotational wind, as the key variable representing the dominant behaviour of the flow. This is necessary in order to show that using PV inversion is an improvement on the standard method.

We use the nonlinear shallow water equations on a sphere. Most meteorological textbooks (eg Haltiner et al 1980) show that through a scale analysis, key non-dimensional numbers are found whose values characterize the flow. One such dimensional number is the Burger number. Cullen (2002) showed that in a high Burger regime, the shallow water equations (SWE) approximate a balanced model called 2D Euler in the asymptotic limit as the Burger number gets much larger than unity. In this balanced model the absolute vorticity, a scalar quantity describing the amount of rotational wind, is materially conserved by the flow. If we are dealing with shallow water flow in a regime where it behaves similarly to inviscid incompressible 2D Euler, it would be sensible to approximate the dominant aspects of the shallow water flow by a key variable of the 2D Euler

model, namely the streamfunction ψ. This quantity can be diagnosed using a Helmholtz decomposition.

The atmosphere, however, is not always in a regime in which the Burger number is larger than unity; there are situations where the Burger number is much smaller and the appropriate balanced model that approximates the shallow water flow is given by the semi-geostrophic equations. In this balanced model it is the height field that dominates the flow.

Potential vorticity inversion can be used to diagnose the dominant aspects of the flow in regimes in which the Burger number is larger than one and smaller than one, since the potential vorticity is defined by both the streamfunction ψ and the height field h.

We now describe the argument more rigorously by considering the governing equations, their relationship to the inviscid incompressible 2D Euler equations, the Helmholtz decomposition, the relationship of SWE's to semi-geostrophic equations and finally the use of PV inversion.

(*b*) *Governing equations*

The nonlinear shallow water equations take the form:

$$\frac{\partial \mathbf{v}}{\partial t} + \mathbf{v} \cdot \nabla \mathbf{v} + f\mathbf{k} \times \mathbf{v} + g\nabla h = 0 \tag{1}$$

$$\frac{\partial h}{\partial t} + \nabla \cdot (h\mathbf{v}) = 0 \tag{2}$$

where the main variables in this formulation are the height of the fluid, h and the horizontal vector wind $\mathbf{v}$. The acceleration due to gravity, g, is considered to be a constant and the Coriolis parameter, f, on the sphere is a function of latitude only. The horizontal gradient operator is represented by ∇.

The basic analysis of linearised versions of these equations leads to the conclusion that there are three eigenmodes: one Rossby mode and two inertio-gravity modes (Daley, 1991; Gill, 1982; Pedlosky, 1987). For the most part in mid-latitudes, there is a separation in time scales between the slow Rossby modes and fast inertio-gravity modes. As stated earlier, we are interested in choosing variables that demonstrate this dynamical separation.

(*c*) *Relationship of governing equations to incompressible 2D-Euler*

One of the key non-dimensional constants that comes from applying scale analysis to the horizontal momentum equations is the Burger number, B_u, which is defined as the ratio of the Rossby radius of deformation, L_R, and the horizontal characteristic length scale L. Specifically,

$$\begin{aligned} B_u &= \frac{L_R}{L}, \\ L_R &= \frac{\sqrt{gH}}{f}, \end{aligned} \tag{3}$$

where f is a typical value for the Coriolis parameter and H is the characteristic depth of the fluid. Another key non-dimensional constant is the Rossby number

$$R_o = \frac{U}{fL}, \tag{4}$$

where U is the characteristic velocity.

For the shallow water equations, in the asymptotic limit as the Burger number gets large, $B_u >> 1$, where the Rossby number is kept small, $R_o << 1$, the typical spatial differences in depth become increasingly less important compared to the effect of the characteristic depth within equation (2). In this case, the continuity equation effectively degenerates into a 2D incompressibility condition. This enforces a non-divergent flow described by incompressible 2D Euler as

$$\frac{\partial \mathbf{v}}{\partial t} + \mathbf{v} \cdot \nabla \mathbf{v} + f\mathbf{k} \times \mathbf{v} + g\nabla h = 0, \tag{5}$$

$$\nabla \cdot \mathbf{v} = 0. \tag{6}$$

Taking the vertical component of the curl of the momentum equation (5) gives the barotropic vorticity equation

$$\frac{\partial \nabla^2 \psi}{\partial t} + \mathbf{v}_\psi \cdot \nabla \left(f + \nabla^2 \psi \right) = 0, \tag{7}$$

where $\mathbf{v}_\psi$ is the rotational, non-divergent part of the wind and the streamfunction ψ is defined by

$$\nabla^2 \psi = \mathbf{k} \cdot \nabla \times \mathbf{v}. \tag{8}$$

As (7) is a single equation with a single time derivative, it has just one eigenmode which approximates the slow mode of the shallow water equations as the Burger number becomes large. The barotropic vorticity equation is an example of a balanced model, as it is a reduced model that approximates the shallow water equations in the asymptotic limit $R_o << 1$, $B_u >> 1$.

From this equation we see that in this limit the streamfunction is the appropriate variable to approximate the slow dynamics.

(*d*) *Linear balance equation*

A consequence of inviscid incompressible 2D Euler is that if we take the divergence of the momentum equation (5), we are left with the Charney-Bolin balance equation

$$g\nabla^2 h = \nabla \cdot f\nabla\psi - 2J(\mathbf{v}_\psi), \tag{9}$$

where J is the Jacobian operator. For $\mathbf{v}_\psi = (u_\psi, v_\psi)$ in Cartesian co-ordinates the Jacobian operator is defined as $J(\mathbf{v}_\psi) = \frac{\partial u_\psi}{\partial x}\frac{\partial v_\psi}{\partial y} - \frac{\partial u_\psi}{\partial y}\frac{\partial v_\psi}{\partial x}$.

Applying scale analysis to this equation shows that for $R_o << 1$ two terms are typically a factor of ten larger than the rest. Taking these two terms on their own gives the linear balance equation as

$$g\nabla^2 h = \nabla \cdot f\nabla\psi. \tag{10}$$

This is a linear mass-wind coupling that naturally takes into account the latitudinal variation of the Coriolis parameter and is useful when length scales $L = 10^6 m$ are considered, even if it is unable to recognise any balanced divergent components.

(e) *Helmholtz decomposition*

A way to approximate the evolution of the barotropic vorticity equation is to evolve the shallow water equations and calculate the rotational, non-divergent part of the wind. This can be achieved using a Helmholtz decomposition, which splits the horizontal wind into a rotational, non-divergent part $\mathbf{v}_\psi$ and a divergent, irrotational part $\mathbf{v}_\chi$ such that

$$\mathbf{v} = \mathbf{v}_\psi + \mathbf{v}_\chi. \tag{11}$$

The rotational winds are defined through the streamfunction in the usual way by

$$\mathbf{v}_\psi \quad = \quad \mathbf{k} \times \nabla\psi.$$

Operational data assimilation systems separate the mass and wind into parts that approximate the Rossby slow mode and two inertio-gravity modes. Most of these systems use the Helmholtz decomposition to approximate the evolution of the streamfunction ψ on each horizontal level and hence, together with the linear balance equation, separate and identify the mass-wind contribution to the slow Rossby mode. The separation is assumed to be accurate across all Burger regimes.

(f) *Relationship of governing equations to semi-geostrophic shallow water equations*

In the shallow water context, the assumption that the streamfunction represents the slow mode becomes increasingly less accurate as the Burger number becomes smaller, $B_u << 1$, while the Rossby number remains small, $R_o << 1$. When the value of the Burger number is smaller than unity it is more appropriate to choose semi-geostrophic shallow water equations as the reference balanced model than inviscid incompressible 2D Euler. This is because it is a more accurate approximation in this regime. The smaller the Burger number, the closer the behaviour of the shallow water equations is to the semi-geostrophic shallow water equations. Further details of the semi-geostrophic shallow water equations can be found in Cullen (2002). It is sufficient to say that all the terms in the continuity equation are important and that this equation no longer reduces into an incompressibility condition. For a small Burger number less than one, the depth fields produced by the standard shallow water equations and the semi-geostrophic shallow water equations are similar, as are the qualitative features of semi-geostrophic and Ertel potential vorticities. In contrast, the rotational wind aspects of the two models differ substantially.

(g) *Linearisation, linearisation states and the LB method*

In data assimilation we are interested in an incremental linearised formulation. We define our increments as the difference between the full heights and linearisation states. In particular, the height and wind increments are defined by

$$\begin{aligned} h' &= h - \overline{h}, \\ \mathbf{v}' &= \mathbf{v} - \overline{\mathbf{v}}, \end{aligned}$$

where the prime variables denote increments and overlined variables represent linearisation states. In this paper, due to limitations of the numerical method, the linearisation states $\overline{h}, \overline{u}, \overline{v}$ are a function of latitude only. The way linearisation states are chosen depends on the situation, but in all cases there is a consistency between the values given to the linearisation states.

The linear equations introduced prior to this section all hold both for increments and for linearisation states, as well as for full fields. In particular, equation (8) can be used to identify ψ' from $\mathbf{v}'$ and $\overline{\psi}$ from $\overline{\mathbf{v}}$.

The streamfunction increment can be considered to represent the balanced part of the incremental flow and the linear balance equation (10) can be used to find the balanced height increment h'_b from the streamfunction increment ψ'. This method for decomposing the flow is referred to here as the LB method. In summary we state the method as

1. calculate the streamfunction increment from the wind increments using equation (8) and assume it is balanced, i.e. $\psi'_b = \psi'$;
2. use the linear balance equation (10) to derive the associated balanced height increment h'_b and the unbalanced height increment $h'_{ub} = h' - h'_b$.

(*h*) *PV and choice of PV inversion*

Our goal is to find a better way to separate the mass-wind contribution to the slow mode. Instead of assuming that the evolution of the slow mode is represented by the evolution of the streamfunction, we assume instead that it is approximated by the evolution of the potential vorticity.

Potential vorticity, q, is considered to be a key dynamical quantity that can capture atmospheric flow features such as frontogenesis, cyclogenesis and general circulation (Hoskins et al, 1985). In the context of 2D Euler, it can be represented as the Laplacian of the streamfunction. In the shallow water context, its form is a generalisation of 2D Euler and is given by

$$q = \frac{f + \nabla^2 \psi}{h}, \tag{12}$$

with the property that it is conserved such that

$$\frac{\partial q}{\partial t} + \mathbf{u} \cdot \nabla q = 0. \tag{13}$$

The linearised potential vorticity increment q' is defined with respect to a reference state $\overline{q}$ that satisfies the nonlinear potential vorticity equation

$$\overline{q} = \frac{f + \nabla^2 \overline{\psi}}{\overline{h}}, \tag{14}$$

with $\nabla^2 \overline{\psi}$ and $\overline{h}$ being reference states for the relative vorticity and height. Linearising the PV equation (12) about $\overline{q}$ then defines the potential vorticity increment q' as

$$\frac{q'}{\overline{q}} = \frac{\nabla^2 \psi'}{f + \nabla^2 \overline{\psi}} - \frac{h'}{\overline{h}}. \tag{15}$$

To invert the potential vorticity increment and obtain a streamfunction and height increment, we need an additional equation. We choose to use the linear balance equation, corresponding to the choice of most operational data assimilation centres for this task, but use it in a different way. Instead of assuming that the streamfunction increment represents the slow mode and using the linear balance equation to find a consistent height (mass), we propose to derive height and wind increments that are consistent with each other in that they conserve the potential vorticity increment while at the same time satisfying the linear balance relation.

(*i*) *The PV method*

The following coupled system of partial differential equations (PDE)s, derived from (15) and (10), defines our decomposition of the slow dynamics:

$$\nabla \cdot f\nabla\psi_b' - g\nabla^2 h_b' = 0, \tag{16}$$

$$\nabla^2\psi_b' - \overline{q}h_b' = \overline{h}q', \tag{17}$$

which we solve, simultaneously for ψ_b' and h_b', where $\overline{q}$, $\overline{h}$ and q' are known. The term $\overline{h}q'$ is precalculated from ψ' and h' by just rearranging equation (15) as

$$\overline{h}q' = -\overline{q}h' + \nabla^2\psi'. \tag{18}$$

In addition, $\nabla^2\psi'$ is obtained from the full wind increments $\mathbf{v}'$ using the equation $\nabla^2\psi' = \mathbf{k}\cdot(\nabla\times\mathbf{v}')$.

The coupled system (16), (17) defines a balanced height increment h_b' and a balanced wind increment, given by $\mathbf{v}_b' = \mathbf{k}\times\nabla\psi_b'$. The balanced wind increment is non-divergent and approximates the full rotational wind increment for high Burger number regimes. The rest of the rotational wind is described as having no potential vorticity increment and conserving a departure from linear balance. The unbalanced rotational wind can be obtained in one of two ways, either by subtracting the balanced wind and height from the full rotational wind and height, or by explicitly solving the simultaneous system

$$\nabla \cdot f\nabla\psi_{ub}' - g\nabla^2 h_{ub}' = \nabla \cdot f\nabla\psi' - g\nabla^2 h', \tag{19}$$

$$\nabla^2\psi_{ub}' - \overline{q}h_{ub}' = 0, \tag{20}$$

where the unbalanced rotational wind is defined to be $\mathbf{v}_{ub}' = \mathbf{k}\times\nabla\psi_{ub}'$. The unbalanced height is denoted by h_{ub}' and again, on the right hand side, we use known full increments ψ' and h'. The equivalence of the two methods to calculate the unbalanced height and unbalanced rotational wind is readily seen by adding equation (16) to (19) and (17) to (20), to give

$$\nabla \cdot f\nabla\left(\psi_b' + \psi_{ub}'\right) - g\nabla^2\left(h_b' + h_{ub}'\right) = \nabla \cdot f\nabla\psi' - g\nabla^2 h', \tag{21}$$

$$\nabla^2\left(\psi_b' + \psi_{ub}'\right) - \overline{q}\left(h_b' + h_{ub}'\right) = \overline{h}q'. \tag{22}$$

The remaining wind increment, namely the divergent part $\mathbf{v}_\chi{}'$, is stored in the velocity potential χ', which is defined as

$$\nabla^2\chi' = \nabla\cdot\mathbf{v}'. \tag{23}$$

We have chosen to solve the coupled system, (16)/(17) (respectively (19)/(20)) directly and to use a finite difference approach. This has the benefit of allowing us to deal with just second order partial differential operators and well as making it easier to find appropriate boundary conditions.

This method of applying a PV inversion to obtain balanced height, h_b', and balanced horizontal winds, $\mathbf{v}_b'$, is referred to here as the PV method. In summary, we state the method as

1. assume that, instead of conserving ψ' as in the LB method, the increment $\overline{h}q'$ is conserved.
2. solve the linear balance and linearised PV equations (16), (17) simultaneously to give balanced streamfunction increments ψ_b' and balanced height increments h_b'; derive the unbalanced height h_{ub} from $h_{ub} = h - h_b$.

(*j*) *Dynamic dependence of linearised potential vorticity on Burger regime*

It is now appropriate to describe the effect of different Burger regimes on linearised potential vorticity and linear balance increments. We consider properties of height, vorticity (the Laplacian of the streamfunction) and potential vorticity increments that satisfy both the linearised potential vorticity relationship (15) and the linear balance equation, (10) when the Coriolis term is constant. It is valid to consider relative vorticity perturbations $\nabla^2\psi'$ since the linear balance equation (10) for constant $f = f_0$ is equal to

$$g\nabla^2 h' = f_0\nabla^2\psi'. \tag{24}$$

Let us assume that the height and vorticity perturbations are on a Cartesian grid for consistency in assuming constant f and assume that these perturbations and the reference linearisation states are known.

We use the relationship (24) between the perturbation in relative vorticity and the height to derive a relationship between the potential vorticity perturbation and the height. We consider perturbations in the height and the vorticity that take the form $h' = \hat{h}e^{i(k_1x+k_2y-\sigma t)}$, $\zeta' = \nabla^2\psi' = \hat{\zeta}e^{i(k_1x+k_2y-\sigma t)}$, where k_1 is the wave number in the x direction, k_2 is the wave number in the y direction and σ is the frequency. Also, we assume that the perturbations satisfy (24). Using these two assumptions,

$$\nabla^2\psi' = -\frac{(k_1^2 + k_2^2)gh'}{f_0}. \tag{25}$$

If the characteristic length scale L is considered to be equal to $(k_1^2 + k_1^2)^{-\frac{1}{2}}$, then the Burger number is equal to $(k_1^2 + k_1^2)^{\frac{1}{2}}(g\overline{h})^{\frac{1}{2}}/f$, where the characteristic height scale H is considered to be equal to $\overline{h}$. By using (15), (25), two separate relationships can be determined (Wlasak, 2002): one defines scaled perturbations in potential vorticity in terms of scaled perturbations in height; the other shows how perturbations in scaled relative vorticity perturbations are related to scaled perturbations in potential vorticity. These relationships are given by

$$\frac{q'}{\overline{q}} = -N\frac{h'}{\overline{h}} \qquad \left(1 - \frac{1}{N}\right)\frac{q'}{\overline{q}} = \frac{\nabla^2\psi'}{\nabla^2\overline{\psi} + f_0} \tag{26}$$

with

$$N = 1 + \frac{f_0\ B_u^2}{f_0 + \nabla^2\overline{\psi}}. \tag{27}$$

As the Burger number is always greater than zero, for any given perturbation, N is always greater than 1. For a fixed $q'/\overline{q}$ and $N >> 1$, $h'/\overline{h}$ will not contribute much to the scaled potential vorticity perturbations; the potential vorticity perturbations are similar to the absolute vorticity perturbations with $q'/\overline{q} \approx \nabla^2\psi'/(f_0 + \nabla^2\overline{\psi})$. Moreover, the greater the value of N, the more similar $q'/\overline{q}$ will be to $\nabla^2\psi'/(f_0 + \nabla^2\overline{\psi})$. The equation (27) shows that a number of conditions can make N large. One possible way, assuming $(f_0 + \nabla^2\overline{\psi})$ to be constant, is to produce a large Burger number. A large Burger number will be obtained when $\overline{h}$ is large or when f_0 is small. In summary, it is expected that for large Burger number $q'/\overline{q}$ will be dominated by $\nabla^2\psi'/(f_0 + \nabla^2\overline{\psi})$.

The equations (26) and (27) can also be written as

$$\left(1 - \frac{1}{P}\right)\frac{q'}{\overline{q}} = -\frac{h'}{\overline{h}} \qquad \frac{q'}{\overline{q}} = P\frac{\nabla^2\psi'}{f_0 + \nabla^2\overline{\psi}} \tag{28}$$

with

$$P = 1 + \frac{f_0 + \nabla^2\overline{\psi}}{f_0 B_u^2}. \tag{29}$$

Examination shows that for a small Burger number, $P >> 1$ with $q'/\overline{q} >> \nabla^2\psi'/(\nabla^2\psi' + f_0)$ and $q'/\overline{q} \approx h'/\overline{h}$. In this situation it is the scaled height perturbations $h'/\overline{h}$ that will dominate $q'/\overline{q}$. Small Burger number regimes will occur where the Coriolis parameter f_0 is not small as in the mid-latitudes and where $\overline{h}$ is small. It is in these regions that the potential vorticity perturbations will most resemble the height perturbations.

3. Numerical Procedure

(*a*) *Preamble*

Our aim is to diagnose the balanced and unbalanced contributions to the mass and wind increments determined by the LB and PV methods and to compare the results under different Burger regimes. We apply the methods on a hemisphere. This is achieved by solving for the fields on the full sphere, making the height field and zonal wind field symmetric about the equator and making the meridional wind antisymmetric. Both shallow water equations on the rotating sphere and the equations (16)-(17) have the geometric property that they conserve these symmetries provided the initial fields have them.

We choose the linearisation states to be a function of latitude only. This makes the coupled equation set separable, enabling the use of a method developed by Moorthi and Higgins (1993) for solving numerically separable elliptic equations. The assumption that the potential vorticity linearisation state is a function of latitude only is a reasonable assumption when the data is coming from a global shallow water model. Except for around the equator, the major contributor to the absolute vorticity is the Coriolis parameter, which is a function of the latitude only. Also the change in height field at any given latitude seems to vary between 5 % and 20 % of its average value.

(*b*) *Longitudinal/Latitudinal decoupling*

The PV method uses 1-dimensional inverse fast Fourier transforms (IFFTs) zonally to decouple the system of partial differential equations (16)-(17) into a series of coupled systems of ordinary differential equations dependent on zonal wavenumber. As the equations we are dealing with are linear, each coupled system of ordinary differential equations is solved independently using second-order finite differences. The final step applies fast Fourier transforms (FFTs) to reconstitute the solution in the physical domain to give balanced height h_b and streamfunction ψ_b.

This method has a number of advantages. Since the ordinary differential equations (ODEs) to be solved for each wavenumber are independent of each other, they can be solved in parallel, making this method quite efficient. Memory requirements are relatively low. The equation should be less sensitive to error as

we are solving coupled systems of ODEs, instead of a highly sensitive fourth order PDE. The coupled system is coded in Matlab, giving the opportunity to use the inbuilt Fourier transform algorithms (Cooley et al, 1965; Frigo et al, 1998).

For clarity, the technique used to solve the coupled system is shown from a continuous perspective, the discrete equivalent being described only where necessary.

We assume a solution of the form

$$\begin{aligned} h'_b(\lambda,\phi) &= \sum_{k=-M/2}^{k=M/2} \widetilde{h}(k,\phi)e^{ik\lambda}, \qquad (30)\\ \psi'_b(\lambda,\phi) &= \sum_{k=-M/2}^{k=M/2} \widetilde{\psi}(k,\phi)e^{ik\lambda},\\ \overline{h}q'(\lambda,\phi) &= \sum_{k=-M/2}^{k=M/2} \widetilde{\overline{h}q'}(k,\phi)e^{ik\lambda}, \end{aligned}$$

with M being an even integer setting a truncation limit to the Fourier approximation, k the wavenumber, and $i=\sqrt{-1}$. Since we have periodicity in the longitudinal direction, λ is discretised as

$$\lambda_j = ja\left(\frac{2\pi}{M+1}\right)\cos\phi, \qquad j=1,...,M+1, \qquad (31)$$

where a is the radius of the earth. The Fourier coefficients $\widetilde{h}(k,\phi)$, $\widetilde{\psi}(k,\phi)$, $\widetilde{\overline{h}q'}(k,\phi)$ are complex.

Substitution of (30) into (16) and (17), produces a series of coupled systems of second order ODEs in ϕ to be solved for variables $\widetilde{h}$, $\widetilde{\psi}$. The system is given for each k by

$$\begin{aligned} -\frac{k^2}{a^2\cos^2\phi}[g\widetilde{h}+f\widetilde{\psi}] + \frac{g}{a^2\cos\phi}\frac{\partial}{\partial\phi}[\cos\phi\frac{\partial\widetilde{h}}{\partial\phi}+f\cos\phi\frac{\partial\widetilde{\psi}}{\partial\phi}] &= 0 \qquad (32)\\ -\frac{k^2}{a^2\cos^2\phi}[\widetilde{\psi}] + \frac{1}{a^2\cos\phi}\frac{\partial}{\partial\phi}[\cos\phi\frac{\partial\widetilde{\psi}}{\partial\phi}] - \overline{q}\widetilde{h} &= \widetilde{\overline{h}q'}. \qquad (33) \end{aligned}$$

In this situation, we have $M+1$ different complex coefficients for $\widetilde{h}$, $\widetilde{\psi}$, $\widetilde{\overline{h}q'}$ which are all functions of latitude λ_j and wave number k. Coefficients $\widetilde{\overline{h}q'}$ are known and $\widetilde{h}$, $\widetilde{\psi}$ are to be determined.

The system (32)-(33) is to be solved for each wavenumber k considered. The beauty of the separability of the coupled PDE's is now apparent; since $\overline{h}$, $\overline{q}$, $\overline{\psi}$ are functions of latitude only, there is no interaction of wavenumber coefficients and each system of ODEs for each wavenumber is solved independently.

(c) *Boundary conditions*

To solve this system we need $\widetilde{\overline{h}q'}(k,\phi)$, which is derived by applying the Fourier transform to the increment $\overline{h}q'(\lambda,\phi)$, given by (18). We obtain

$$\widetilde{\overline{h}q'}(k,\phi) = \frac{1}{M+1}\sum_{j=1}^{j=M+1} \overline{h}q'(\lambda_j,\phi)e^{-ik\lambda_j}, \qquad k=-M/2,\cdots,M/2. \tag{34}$$

Dirichlet boundary conditions are set at the poles for $k \neq 0$ with

$$\begin{aligned} &\widetilde{h}_b(k,\pi/2)=0, && \widetilde{h}_b(k,-\pi/2)=0,\\ &\widetilde{\psi}_b(k,\pi/2)=0, && \widetilde{\psi}_b(k,-\pi/2)=0. \end{aligned} \tag{35}$$

For $k=0$ we solve (33) over the sphere and enforce a zero value at the equator for the anti-symmetric balanced streamfunction increment difference. A global uniqueness condition is used of the form,

$$\int \widetilde{h}_b dS \;=\; 0, \tag{36}$$

which is rewritten as

$$\int_{-\frac{\pi}{2}}^{\frac{\pi}{2}} \widetilde{h}_b(0,\phi)\cos\phi d\phi \;=\; 0. \tag{37}$$

The global uniqueness condition applied to $\widetilde{\psi}$,

$$\int_{-\frac{\pi}{2}}^{\frac{\pi}{2}} \widetilde{\psi}_b(0,\phi)\cos\phi d\phi \;=\; 0, \tag{38}$$

is automatically satisfied due to the imposed anti-symmetric nature of the integrand. Once (32)-(33) has been solved for all wavenumbers considered, we synthesise the complex coefficients using a discrete inverse Fourier transform.

(d) *Scaling*

A scaling is introduced to make terms in the discretised operator of approximately the same size. Scaling of equations is important so as to eliminate unnecessary sensitivity to numerical error in the problem. We wish to choose a scaling that produces a coupled system of ODEs that are represented by a positive definite matrix. Such a matrix guarantees a unique solution to the discrete problem. This scaling is achieved using a combination of scale analysis and a control volume approach. The control volume technique in this situation amounts to multiplying the value at each grid point in Fourier space by its associated weighted grid-spacing. For non-polar grid points, the weighted grid-spacing is approximated by $2\pi a^2\Delta\phi\cos\phi_i$, where a is the radius of the earth, ϕ_i is the value of the latitude at a grid point and $\Delta\phi$ is the grid spacing. The weighted grid-spacing is an $O(\Delta\phi^2)$ approximation to the true surface area of a spherical segment. At the poles the surface area is given by $2\pi a^2\frac{\Delta\phi}{2}\cos\phi_{\frac{1}{2}}$ where $\phi_{\frac{1}{2}}$ is the latitude value mid-way between the pole and the adjacent point. The discretisation at the poles is derived using Green's theorem as detailed by Barros (1991).

The proposed additional scaling involves a change from height to geopotential height and from streamfuction to streamfunction multiplied by the angular velocity of the earth, 2Ω. These scalings make the terms in the modified equations roughly of the same magnitude.

(*e*) *The discrete system*

The inverse discrete Fourier transforms take the values of M spatial points at each given latitude and convert to $M/2+1$ wavenumber coefficients, one for each wavenumber including $k=0$. Thus we have $M/2+1$ discrete ODE systems that are solved using traditional second-order centered finite differences.

The discrete ODE system for each wavenumber k has a block tridiagonal structure and can be represented in the form $A\mathbf{x}=\mathbf{b}$ with A being a $(2N-4)\times(2N-4)$ block tri-diagonal nonsingular matrix, where N is the number of equally spaced grid points from north pole to south.

For $k=0$ the situation is a little more complex. At the poles we set homogenous Neumann boundary conditions for both variables, which fix both fields up to the addition of a constant. Additional boundary conditions are applied to both variables. The streamfunction is assumed to be a continuous smooth function and must be zero at the equator due to the balanced streamfunction being anti-symmetric. At the equator, for $k=0$, we do not solve the coupled system as its stands but instead solve one equation in which the coupled equations have been added together. This single equation at the equator is discretised using fourth order centered differences.

An antisymmetric solution about the equator in balanced streamfunction enforces a symmetric solution in balanced height h_b and there is no need to enforce $\frac{\partial h_b}{\partial \phi}=0$. Instead a discrete approximation to mass conservation is enforced, so that the balanced height field represents the same mass as the full height increment difference.

A unique solution is given, provided a compatibility condition is enforced on the full potential vorticity increment such that the volume-weighted sum of the discrete increments $\overline{h}q'$ over the sphere is equal to zero (Swarztrauber,1974). This is automatically achieved due to the antisymmetric nature of the full potential vorticity increment.

4. Results

We investigate whether the PV method provides a better representation of balanced and unbalanced control variables than the LB method. If the coupled PV system is behaving properly, then in high Burger regimes the balanced streamfunction increment ψ'_b should be similar to ψ'. Similarly, at low Burger regimes the balanced height increment should resemble the full height increment. We perform two sets of experiments: the first testing the PV and LB methods against a primarily balanced flow defined by the evolution of a Rossby-Haurwitz wave; the second testing the methods with height and wind increments that are essentially unbalanced.

For the first set of experiments, appropriate height and wind fields need to be generated to test the coupled system. A global SWE model is run, using a Rossby-Haurwitz wave (RH wave) as an initial condition. The RH wave is defined in the Appendix through an analytic expression and is used in standard test cases as an initial condition for testing global SWE models (Williamson et al, 1992). It has the property that the wind pattern is advected meridionally at a constant angular velocity on the sphere when propagated under incompressible 2D Euler equations. When used in the SWE context such behavior occurs in a regime where $B_u >> 1$, the characteristic height H is large and there is little divergent wind. The defining

parameters of the wave are given by the wavenumber R and the base height h_0 of the wave at the poles. The strength of the underlying zonal wind from west to east is given by ω and K controls the amplitude of the wave. In this test we set $R = 4$, $K = \omega = 7.847e^{-7}s^{-1}$, $h_0 = 8000$. Approximating the characteristic length scale by $L = 2a\pi \cos\phi \ /(4R)$ m, produces Burger values $B_u = 1.8$ at $\phi = 60°$, $B_u = 1.6$ at $\phi = 45°$ and $B_u = 4.6$ at $\phi = 10°$, where ϕ denotes the latitude.

The global SWE model uses a semi-implicit semi-Lagrangian scheme similar to that used in the Met Office Unified Model (vn 5.1) (Malcolm, 1996). It has the property that it conserves symmetry and antisymmetry about the equator given appropriate symmetric/antisymmetric initial fields.

The model is run for 24 hrs, with a timestep of 0.5 hr at coarse spatial resolution with grid spacing $\Delta\phi = a\pi/64$, and $\Delta\lambda = a\pi/48$ with the height and wind components stored from the end of the time integration. These fields are zonally-averaged to give the linearisation states. The increments are defined by the difference between the full fields and the zonally-averaged fields. The discrete version of the nonlinear PV equation (14) is used to define the latitudinally dependent PV linearisation state $\overline{q}$. The quantity $\overline{h}q'$ that is needed is given by (18).

The PV method produces both balanced height and streamfunction increments. Figure 1 compares the balanced streamfunction to the respective full field over the area $(\phi \in [\pi/2, -\pi/2]) \times (\lambda \in [0, \pi/2])$.

Figure 1. Balanced ψ (left) and full ψ (right) for RH wave propagated 1 day at high Burger number, for $(\phi \in [\pi/2, -\pi/2]) \times (\lambda \in [0, \pi/2])$ (scale denotes grid points)

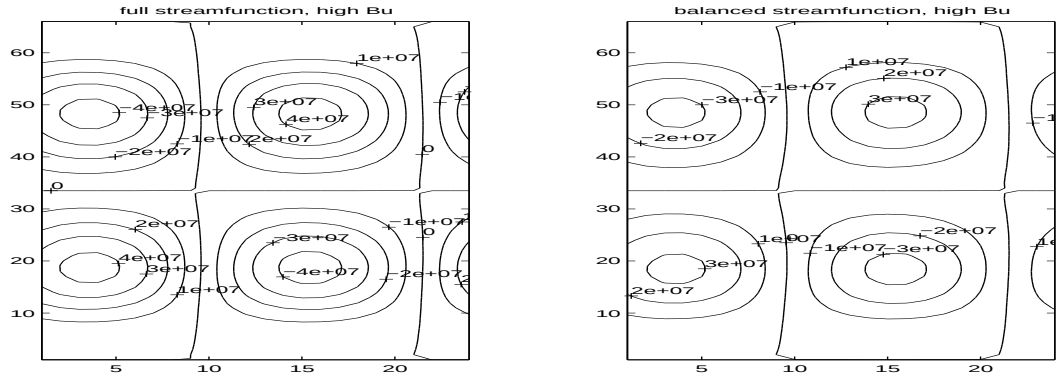

The two fields are qualitatively similar in shape. The balanced streamfunction has an amplitude approximately 80% of the full ψ field. Also the balanced field is slightly more diffuse. In comparision, the balanced height and the full height perturbations in Figure 2 are notably different in shape.

The above experiment is repeated with RH wave parameters set to $R = 4$, $K = w = 7.847 \times 10^{-7}\ s^{-1}$ and $h_0 = 50\ m$. This produces a low Burger regime in the mid-latitudes. The value for the Burger number is $B_u = 0.21$ at $\phi = 60°$, with $B_u = 0.22$ at $\phi = 45°$ and $B_u = 0.84$ at $\phi = 10°$. A high spatial resolution is used with $\Delta\phi = \pi/128$, $\Delta\lambda = \pi/192$. Other model parameters are kept the same. As seen in Figure 4, in regions such as the mid-latitudes, where B_u is low, the balanced height perturbations resemble the full height perturbations. The full

Figure 2. Balanced height perturbations (left) and full height perturbations (right) for RH wave propagated 1 day at high Burger number, with $(\phi \in [\pi/2, -\pi/2]) \times (\lambda \in [0, \pi/2])$ (scale denotes grid points)

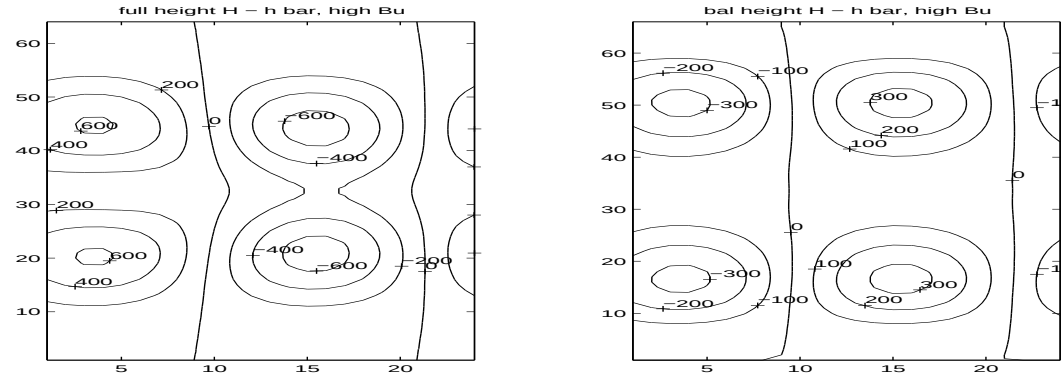

Figure 3. Balanced ψ (left) and full ψ (right)for RH wave propagated 1 day at low Burger number, with $(\phi \in [\pi/2, -\pi/2]) \times (\lambda \in [0, \pi/2])$ (scale denotes grid points)

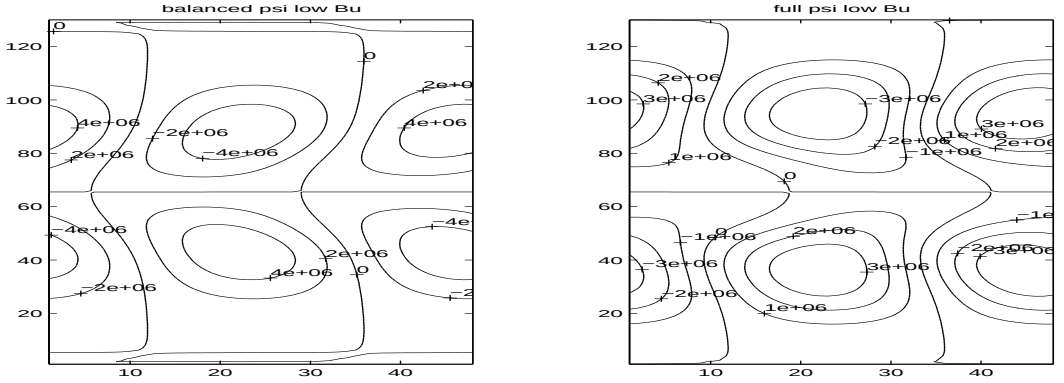

Figure 4. Balanced height (left) and full height (right) for RH wave propagated 1 day at low Burger number, with $(\phi \in [\pi/2, -\pi/2]) \times (\lambda \in [0, \pi/2])$ (scale denotes grid points)

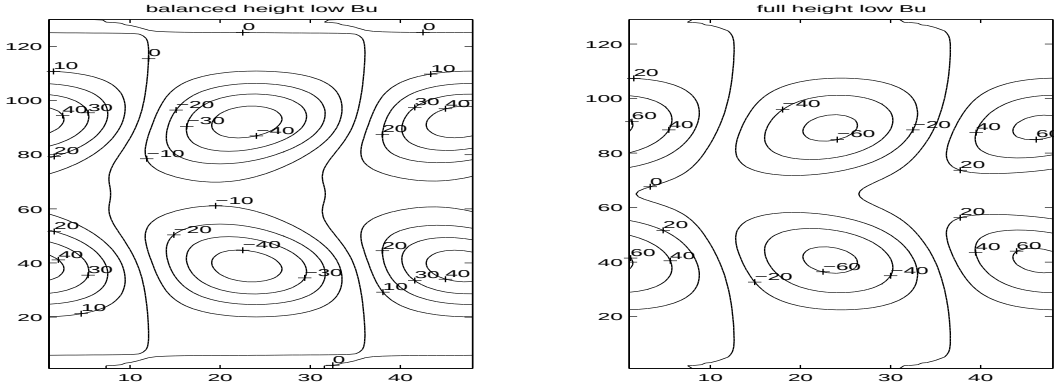

streamfunction and its respective balanced field are far less similar to each other. This is seen in Figure 3.

The Rossby-Haurwitz wave is an idealistic wave to consider; the wave is smooth and is analytically defined. We now consider a more realistic situation by applying the methods to increments derived from a real data set $INI7C$. These are produced by taking the initialised fields produced by a potential vorticity conserving initialisation scheme and subtracting them from the corresponding uninitialised field. The uninitialised field is obtained from a spherical harmonic description of the observed fields at T106 resolution from a NETCDF file $VDG7.13.cdf$, kept at NCAR and found in $ftp://ftp.cgd.ucar.edu/pub/jet/shallow/nminit/$. This experiment shows the strengths and weaknesses of the control variables that we have developed.

Figure 5 shows the height and wind increments used to test the control variables. A stereographic projection is used centred on the North Pole. The increments are composed of many different waves on a wide range of length scales. The wind increments are typically between $-8ms^{-1}$ and $8ms^{-1}$ and the height increments vary between $-60m$ and $60m$. It is also clear from the figure that there is great variability in the flow with waves of both short and long wavelengths present.

If the initialisation is perfect then the increments consist of just the unbalanced flow. A perfect set of control variables would apportion the flow into the two unbalanced variables. In practice this does not occur. Since the balanced condition used by both sets of control variables holds for the f-plane SWEs linearised about a state of rest, the methods can only approximate the exact balanced and unbalanced parts of the nonlinear flow. In fact, provided the initialisation is perfect, the performance of the balanced control variables is determined by their relative size; the balanced control variables that correspond to the smallest balanced height and wind increments identifies the better set.

A coarse grid with $\Delta\phi = \pi/64$ and $\Delta\lambda = \pi/48$ is used for this test. The linearisation state U is shown in the bottom right corner of Figure 5. It is calculated by applying the PV method to longitudinally averaged uninitialised fields and then using the 2D Helmholtz relation to convert the resulting streamfunction to a wind component. This method also calculates a height field that is used to provide the latitudinally varying linearisation state. The linearisation states for low and high Burger regimes are shown in Figure 6. The high Burger regime has $B_u \approx 3.33$ at $\phi = 45°$. The mean height of the linearisation state is 11 km. The low Burger regime is given by reducing the mean height of the linearisation state to 41 m at the poles. This gives a Burger number less than unity above $\phi = 45°$ and makes the sum of the increment and the linearisation states non-negative. The linearisation states of the winds are unchanged.

Figures 7 and 8 show the balanced height and wind increments produced by the LB and PV methods in the high Burger regime. The balanced winds from the two methods are dissimilar. The balanced winds from the PV method are much smaller. This is because the scaled potential vorticity increment $\overline{h}q'$ does not resemble the full vorticity increment $\nabla^2\psi'$. There is cancellation between $\nabla^2\psi'$ and $\overline{q}h'$. This makes the scaled linearised potential vorticity increments $\overline{h}q'$ a factor of ten smaller than the vorticity increment $\nabla^2\psi'$. This shows that the PV method is performing better than the LB method at producing balanced fields.

Figure 5. (Top) U and V wind increments produced using test case $INI7C$, (bottom right) height increment using test case $INI7C$, (bottom left) U field linearisation state

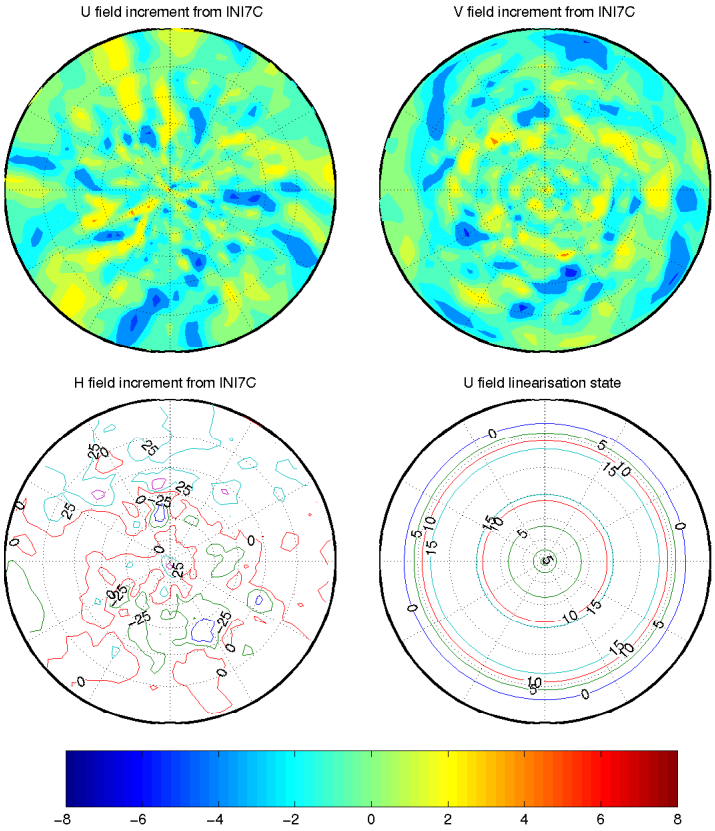

Figure 6. H field linearisation states for low Burger regime (left) and high Burger regime (right)

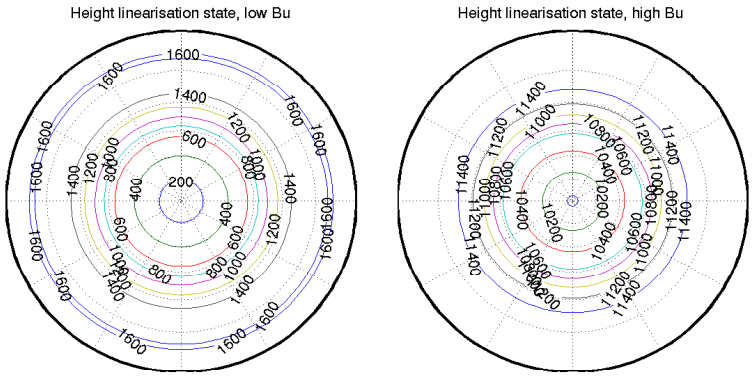

Figure 7. (Top left) Height increment produced using test case $INI7C$. (Top right) balanced height increment produced by LB method. (Bottom left) Balanced height increment using PV method at low B_u. (Bottom right) Balanced height increment using PV method at high B_u

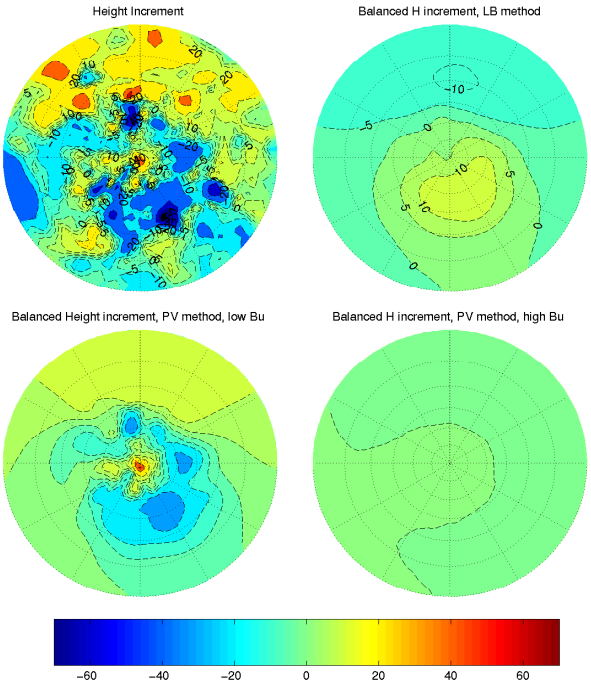

Figure 8. Balanced wind increments produced by using the LB and PV methods at high Bu (mean height $H \approx 11km$)

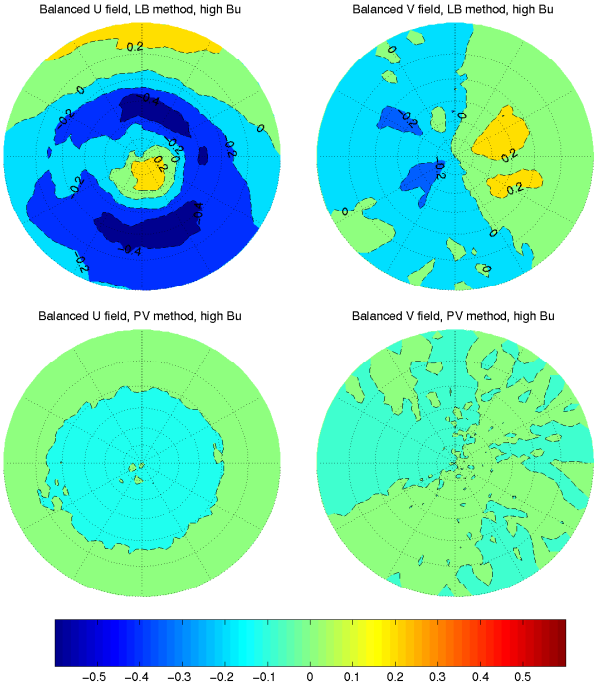

In the low Burger regime, the effect of reducing the mean height of the flow means that the increment that was previously generated to be unbalanced in a high Burger regime of mean depth of 11 km can no longer be considered to be unbalanced, as potential vorticity is regime dependent. All that can be claimed theoretically is that the balanced contribution should resemble the full height increment in the PV method due to being in a low Burger regime. This indeed happens as can be seen in the bottom left picture of Figure 7. The LB method, being insensitive to the Burger regime, produces the same balanced increments as before in the high Burger regime.

It is interesting to note that around the equator, the LB and PV methods are not producing similar results even though a high Burger regime is always present within this region. This is due to the unbalanced height increment still contributing to the scaled potential vorticity within these regions.

5. Conclusions

We propose a new PV-based approach to the separation of balanced and unbalanced flow that incorporates flow regime dependence. The benefits of this approach are demonstrated theoretically and experimentally in the context of the shallow water equations. The results concur with findings produced by Cullen (2003) in which a similar technique was applied in a dimensional context to the reformulation of the background error covariance within a four-dimensional data assimilation system. Although Cullen's method had difficulties in dealing with spurious modes produced by the vertical-staggered Lorenz grid used at ECMWF at the time, the findings from both studies are encouraging.

As shown here, the PV-based method at high Burger number produces control variables that are similar to those produced by the customary streamfunction-constrained LB method. At low Burger number the PV method produces control variables in which the full height increments/perturbations dictate the balanced height and wind fields. A difficulty arises in using a linearised potential vorticity increment at very low Burger number. The smaller the height linearisation state, the less accurate the linearisation of the potential vorticity increment becomes. Despite this problem, balanced height increments are obtained that follow the theory in that at low Burger number the balanced height increments resemble the full height increments. Similarly, for a high Burger regime the balanced streamfunction perturbations resemble the full streamfunction perturbations as seen in the Rossby-Haurwitz wave.

Acknowledgements

This work has been made possible through an EPSRC research studentship CASE award supported by the Met Office. We also thank Mike Cullen for useful discussions of the topic.

Appendix

Rossby-Haurwitz wave on the sphere

The Rossby-Haurwitz wave is characterised by parameters a, g, Ω, R, h_0, ω and K, where a is the radius of the sphere, g is the acceleration due to gravity, R is the wave number and h_0 is the height at the poles. The strength of the underlying

zonal wind from west to east is given by ω and K controls the amplitude of the wave. The latitude and longitude co-ordinates are represented by ϕ and λ.

The initial velocity field is defined as,

$$\begin{aligned} u &= a\omega\cos\phi + aK\cos^{R-1}\phi(R\sin^2\phi - \cos^2\phi)\cos R\lambda, \\ v &= -aKR\cos^{R-1}\phi\sin\phi\sin R\lambda. \end{aligned} \tag{A.1}$$

The initial height field is defined as,

$$h = h_0 + \frac{a^2}{g}[A(\phi) + B(\phi)\cos R\lambda + C(\phi)\cos(2R\lambda)], \tag{A.2}$$

where the variables $A(\phi),\ B(\phi),\ C(\phi)$ are given by

$$\begin{aligned} A(\phi) &= \frac{\omega}{2}(2\Omega+\omega)\cos^2\phi + \frac{1}{4}K^2\cos^{2R}\phi[(R+1)\cos^2\phi \\ &\quad +(2R^2 - R - 2) - 2R^2\cos^{-2}\phi], \\ B(\phi) &= \frac{2(\Omega+\omega)K}{(R+1)(R+2)}\cos^R\phi[(R^2+2R+2) \\ &\quad -(R+1)^2\cos^2\phi], \\ C(\phi) &= \frac{1}{4}K^2\cos^{2R}\phi[(R+1)\cos^2\phi - (R+2)]. \end{aligned} \tag{A.3}$$

References

Barros, S. R. M. 1991 Multigrid methods for two- and three-dimensional Poisson-type equations on the sphere. *J. Comput. Phys.***92** 313-348

Cooley, J. W. and Tukey, J. W. 1965 An Algorithm for the Machine Computation of the Complex Fourier Series. **19**, 297-301

Cullen, M. J. P. 2002 Large-scale non-turbulent dynamics in the atmosphere. *Q. J. R. Meteorol. Soc.* **128**, 2623-2639

Cullen, M. J. P. 2003 Four-dimensional variational data assimilation: A new formulation of the background -error covariance matrix based on a potential-vorticity representation *Q. J. R. Meteorol. Soc.* **129**, 2777-2796

Daley, R. 1991 Atmospheric Data Analysis, Cambridge University Press

Gill, A. E. 1982 Atmosphere-Ocean Dynamics, International Geophysics Series, Volume 30, Academic Press

Haltiner, G. J. and Williams, R. T. 1980 Numerical Prediction and Dynamic Meteorology, 2nd Ed, John Wiley & Sons

Hoskins, B. J., McIntyre, M. E. and Robertson, A. W. 1985 Use and significance of isentropic potential vorticity maps. *Q. J. R. Meteorol. Soc.* **111(470)**, 877-946

Frigo, M., and Johnson, S. G. 1998 FFTW: An Adaptive Software Architecture for the FFT. *Proceedings of the International Conference on Acoustic, Speech, and Signal Processing* **3**, 1381-1384

Lorenc, A. C. 2003 Modelling of error covariances by 4D-Var data assimilation. *Q. J. R. Meteorol. Soc.* **129**, 3167-83

Malcolm, A. J. 1996 Evaluation of the proposed new unified model scheme vs the current unified model scheme on the shallow water equations. *Numerical Analysis Report, Mathematics department, Reading University* **1**

McIntyre, M. E. and Norton, W. 2000 Potential vorticity inversion on a hemisphere. *J. Atmos. Sci.* **57**, 1214 - 1235

Moorthi, S. and Higgins, R. W. 1993 Application of Fast Fourier Transforms to the Direct Solution of a Class of Two-Dimensional Separable Elliptic Equations. *Mon. Wea. Rev.* **121**, 290-296

Pedlosky, J. 1987 'Geophysical Fluid Dynamics', 2nd edition, Springer

Swarztrauber, P. N. 1974 The direct solution of the discrete Poisson equation on the surface of a sphere *J. Comp. Phys* **15**,pp 46-54

Williamson, D. L., and Drake, J. B. 1992 A Standard Test Set for Numerical Approximations to the Shallow Water Equations in Spherical Geometry. *J. Comp. Phys.* **102**, 211-224

Wlasak, M. A. 2002 'The examination of balanced and unbalanced flow using potential vorticity in Atmospheric Modelling'. PhD thesis, University of Reading